DISCOVERY OF A RED GIANT WITH SOLAR-LIKE OSCILLATIONS IN AN ECLIPSING BINARY SYSTEM FROM *KEPLER* SPACE-BASED PHOTOMETRY

S. Hekker[1], J. Debosscher[2], D. Huber[3], M. G. Hidas[3,4,5], J. De Ridder[2], C. Aerts[2,6], D. Stello[3], T. R. Bedding[3],
R. L. Gilliland[7], J. Christensen-Dalsgaard[8], T. M. Brown[4], H. Kjeldsen[8], W. J. Borucki[9], D. Koch[9], J. M. Jenkins[10],
H. Van Winckel[2], P. G. Beck[2], J. Blomme[2], J. Southworth[11], A. Pigulski[12], W. J. Chaplin[1], Y. P. Elsworth[1],
I. R. Stevens[1], S. Dreizler[13], D. W. Kurtz[14], C. Maceroni[15], D. Cardini[16], A. Derekas[3,17], and M. D. Suran[18]

[1] School of Physics and Astronomy, University of Birmingham, Edgbaston B15 2TT, UK; saskia@bison.ph.bham.ac.uk
[2] Instituut voor Sterrenkunde, Katholieke Universiteit Leuven, Celestijnenlaan 200D, B-3001 Leuven, Belgium
[3] Sydney Institute for Astronomy (SIfA), School of Physics, University of Sydney, NSW 2006, Australia
[4] Las Cumbres Observatory Global Telescope, Goleta, CA 93117, USA
[5] Department of Physics, University of California, Santa Barbara, CA 93106, USA
[6] IMAPP, Department of Astrophysics, Radbout University Nijmegen, P.O. Box 9010, 6500 GL Nijmegen, The Netherlands
[7] Space Telescope Science Institute, 3700 San Martin Drive, Baltimore, MD 21218, USA
[8] Department of Physics and Astronomy, Aarhus University, DK-8000 Aarhus C, Denmark
[9] NASA Ames Research Center, MS 244-30, Moffet Field, CA 94035, USA
[10] SETI Institute/NASA Ames Research Center, MS 244-30, Moffet Field, CA 94035, USA
[11] Astrophysics Group, Keele University Newcastle-under-Lyme, ST5 5BG, UK
[12] Instytut Astronomiczny Uniwersytetu Wroclawskiego, Kopernika 11, 51-622 Wroclaw, Poland
[13] Georg-August Universität, Institut für Astrophysik, Friedrich-Hund-Platz 1, D-37077 Göttingen, Germany
[14] Jeremiah Horrocks Institute of Astrophysics, University of Central Lancashire, PR1 2HE, UK
[15] INAF-Osservatorio Astronomica di Roma, via Frascati 3, I-00040 Monteporzio C. (RM), Italy
[16] IASF-Roma, INAF, V. del Fosso del Cavaliere 100, 00133 Roma, Italy
[17] Konkoly Observatory, Hungarian Academy of Sciences, H-1525 Budapest, P.O. Box 67, Hungary
[18] Astronomical Institute of the Romanian Academy, Str. Cutitul de Argint 5, RO 40557, Bucharest, Romania

ABSTRACT

Oscillating stars in binary systems are among the most interesting stellar laboratories, as these can provide information on the stellar parameters and stellar internal structures. Here we present a red giant with solar-like oscillations in an eclipsing binary observed with the NASA *Kepler* satellite. We compute stellar parameters of the red giant from spectra and the asteroseismic mass and radius from the oscillations. Although only one eclipse has been observed so far, we can already determine that the secondary is a main-sequence F star in an eccentric orbit with a semi-major axis larger than 0.5 AU and orbital period longer than 75 days.

Key words: binaries: eclipsing – stars: individual (KIC8410637) – stars: oscillations

1. INTRODUCTION

The prospects for asteroseismology of red giant stars have increased significantly with the launch of *Kepler* (Borucki et al. 2009) in 2009 March and *CoRoT* (Baglin et al. 2006) in 2006 December. These satellites provide uninterrupted long time series of high-precision photometry for a large sample of stars. Among these stars are many red giants, allowing for both statistical analyses and detailed individual studies. *CoRoT* data have already revealed the presence of nonradial oscillation modes in red giants (De Ridder et al. 2009) and have given rise to a population synthesis study (Miglio et al. 2009). The currently available *Kepler* data reveal clear solar-like high radial overtone *p*-mode oscillations in a large sample of red giants, extending in luminosity from the red clump to the bottom of the giant branch (Bedding et al. 2010).

For in-depth studies, including detailed stellar modeling, accurate stellar parameters are needed. Red giants of different masses occupy a narrow region in the H-R diagram, which results in relatively large errors when estimating the mass from measured classical parameters, such as effective temperature, surface gravity and luminosity, and from evolutionary tracks. A better estimate can be obtained from the characteristic frequencies of solar-like oscillations in these stars and their frequency separations, either through modeling or through scaling relations (Kjeldsen & Bedding 1995). Here we use a modeling approach and scaling relations to compute an asteroseismic mass and radius.

Eclipsing binary systems provide the primary method for measuring masses and radii of stars. However, the probability of observing an eclipsing system is low, because of the geometrical restriction that the system has to be viewed close to the orbital plane. We report here the discovery of a pulsating red giant in an eclipsing binary system observed by *Kepler*. This star was found using automated variability classification methods to the targets of the asteroseismology program of *Kepler* (Debosscher et al. 2009; Blomme et al. 2010).

2. OBSERVATIONS

Photometric data for KIC8410637[19] (TYC 3130-2385) have been taken with *Kepler* during the commissioning run (Q0) from 2009 May 2 through 11, and the following first science run (Q1) of 33.5 days. We present results based on these combined time series of about 40 days. This star has a magnitude of 10.77 mag in the *Kepler* bandpass and was selected by the *Kepler* Asteroseismic Science Consortium (KASC, Gilliland et al. 2010) for long-cadence observations. The time series data have a 29.4 minute cadence and show both solar-like oscillations in the frequency regime expected for a red giant and an eclipse (see Figure 1).

---

[19] KIC = Kepler Input Catalog, Brown et al. (2005).
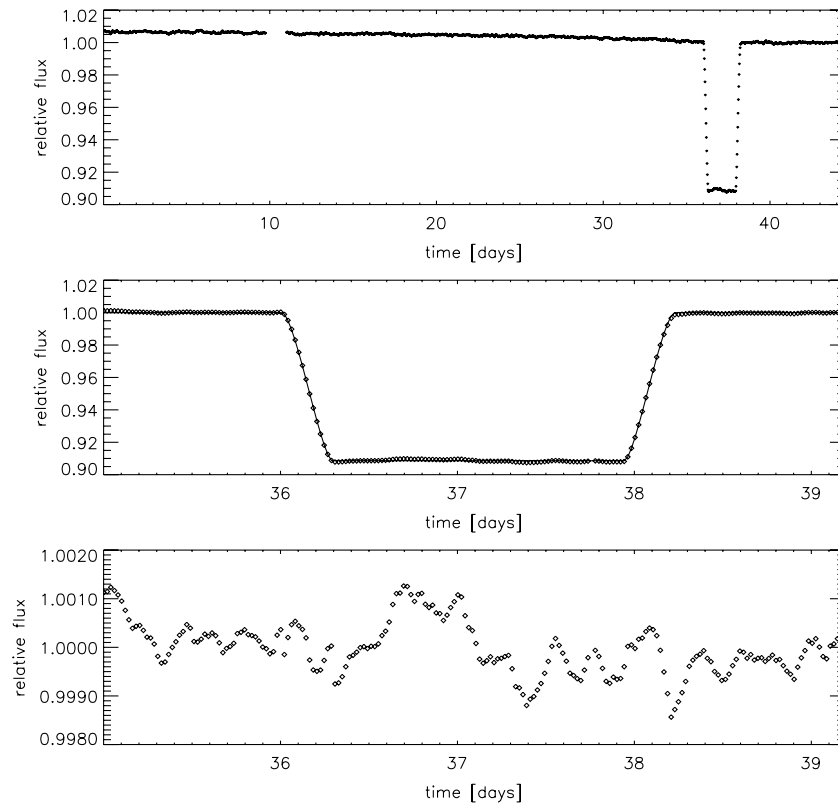
Figure 1. Top: time series data from *Kepler* of KIC8410637. Middle: a section of the light curve centered on the eclipse with the best-fit model (solid line). Bottom: the residuals after correcting for the eclipse model, clearly showing the solar-like oscillations.

This star has also been part of the TrES-Lyr1 ground-based survey[20] (O'Donovan et al. 2006) from which time series photometry with a time span of 75 days is at our disposal. In these data, no eclipse is visible, while the primary and possibly the secondary eclipse (depth predicted in Section 6) would have been detected had they occurred during the time span of the observations. The fact that the primary is not seen in the TrES data implies that the period is longer than the duration of the TrES observations.

This star was also observed photometrically by the Super-WASP cameras (Pollacco et al. 2006) for 100 days in 2007 and for 90 days in 2008. There is a suspicion of a secondary eclipse, but no primary eclipse has been observed during these periods, which have some gaps due to weather conditions. Observations for KIC8410637 are also available from the All Sky Automated Survey (ASAS; Pojmański 1997), in which there are three points that have lower flux than the majority. These points might be due to the eclipse, which would imply an orbital period of about 380 days or a submultiple thereof. Unfortunately, there are too few points, and their uncertainty is too large to draw firm conclusions.

Additionally, we checked whether we could put more constraints on the period from the time stamps of the data we have at our disposal. We determined which periods would have led us to miss primary eclipses because of a lack of observations. We would have missed all eclipses for an orbital period of about 135, 220, 253, 261, 270, and 295 days. All other possible periods are longer than the 380 days mentioned above.

Table 1
Stellar Parameters of KIC8410637

Parameter	KIC	Ofek (2008)	Spectroscopy
T_{eff} (K)	4680 ± 150	4650	4650 ± 80
$\log(g)$ (c.g.s.)	2.8 ± 0.3		2.70 ± 0.15
[Fe/H] (dex)	-0.3 ± 0.3	-0.38	0.0 ± 0.1
$v \sin i$ (km s^{-1})			5.0 ± 0.7
ξ_{micro} (km s^{-1})			1.3 ± 0.1

3. STELLAR PARAMETERS

For KIC8410637, the KIC (Brown et al. 2005) provides a set of stellar parameters, as listed in Table 1. Tycho-2 (Høg et al. 2000) and Two Micron All Sky Survey (Skrutskie et al. 2006) photometry are also available. Ofek (2008) fitted these colors with synthetic photometry of stellar templates (Pickles 1998). Using two methods, Ofek (2008) classified the star as a metal-weak K2III star with an effective temperature of 4650 K or a K4V star with a temperature of 4350 K.

We also obtained three spectra with the HERMES spectrograph (Raskin & Van Winckel 2008) mounted on the Mercator Telescope, La Palma, Spain: two on 2009 October 13 and one on 2009 October 15. These spectra have a resolution of about 85,000 and a wavelength range of 4000–9000 Å. We analyzed the average spectrum, which has a typical signal-to-noise ratio of ∼90 at 6000 Å, with methods described by Hekker & Meléndez (2007) and list the results in the last column of Table 1. This method does not directly provide uncertainties on the individual parameters. Here, we adopted the total of the difference and scatter between the values of Hekker & Meléndez
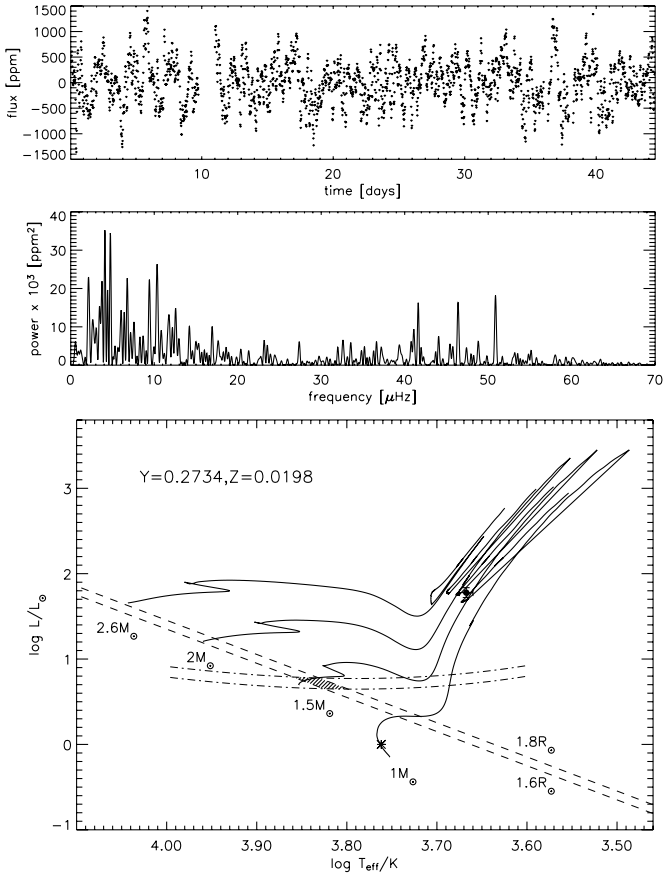
Figure 2. Top: flux as a function of time, after removing the binary signature as described in the text. Centre: the power spectrum of the red giant oscillations. The power excess due to solar-like oscillations is present in the range 30–60 μHz. The excess below 20 μHz might be due to granulation in the primary's atmosphere. Bottom: H-R diagram with BASTI (Pietrinferni et al. 2004) evolutionary tracks for different masses and solar metallicity. The filled circle shows the position of the red giant. The shaded area shows the secondary position constrained by two values derived from the light-curve fit: the radius ratio (dashed lines) and the bolometric luminosity ratio (dashed-dotted lines; taking into account the *Kepler* bandpass). The asterisk indicates the position of the Sun.

(2007) and the values of Luck & Heiter (2007); see Hekker & Meléndez (2007) for more details. For $v \sin i$, we computed the uncertainty from a 10% uncertainty in the total FWHM of the lines, which is combined with the σ on the macro turbulence. These results are in agreement with those in the KIC and the literature. They confirm the red giant nature of the primary star.

We investigated the spectrum for signatures of the secondary star in the form of additional absorption lines and cross-correlation profiles, but no clear signatures could be detected. The three spectra obtained over a time span of three days are not sufficient to see radial velocity variations due to the binary orbit.

4. ASTEROSEISMIC ANALYSIS

Solar-like oscillations are visible both during and outside the eclipse (Figure 1). To analyze these, we adopted two approaches. In the first approach, we corrected the light curve including the eclipse by fitting and subtracting trends for different parts of the time series using a linear polynomial for the commissioning data, a second-order polynomial for the part of the Q1 data before the eclipse, the mean value for the data in full eclipse, and a linear polynomial for the data obtained after the eclipse.

Table 2
Oscillation Parameters of KIC8410637 Computed with Different Methods

Parameter	Octave1	Octave2	Sydney	RADIUS
	–	Measured	–	Model
ν_{max} (μHz)	45.0 $\pm$ 4.8	45.2 $\pm$ 1.3	44.2 $\pm$ 0.5	
$\Delta\nu$ (μHz)	4.64 $\pm$ 0.23	4.5 $\pm$ 0.1	4.51 $\pm$ 0.37	
$\delta\nu_{02}$ (μHz)	0.6 $\pm$ 0.1		0.69 $\pm$ 0.09	
$A_{\ell=0}$ (ppm)	57.6 $\pm$ 7.3	61.8 $\pm$ 6.2	53.4 $\pm$ 1.9	
	–	Derived	–	
R ($R_\odot$)	11.2 $\pm$ 1.6	11.8 $\pm$ 0.7	11.4 $\pm$ 1.9	13.1 $\pm$ 1.7
L ($L_\odot$)	53 $\pm$ 16	58 $\pm$ 8	55 $\pm$ 19	72 $\pm$ 19
M ($M_\odot$)	1.7 $\pm$ 0.7	1.8 $\pm$ 0.3	1.7 $\pm$ 0.9	

We omitted the observations during ingress and egress. The resulting time series is shown in the top panel of Figure 2. In the second approach, we omitted the complete eclipse from the time series.

The Fourier spectrum shows a clear power excess (see the second panel of Figure 2). The power excess is present between 30 and 60 μHz, which is the dominant range of ν_{max} (frequency of maximum oscillation power) found for a large sample of red giants observed by *CoRoT* (Hekker et al. 2009b). This reflects the high population density of red-clump stars, compared to stars on the ascending branch (Miglio et al. 2009). No power excess is present at frequencies between 70 μHz and the Nyquist frequency of ~280 μHz. We analyzed the power spectrum obtained from the corrected time series with two methods of the Octave pipeline (Hekker et al. 2009a: Octave1 and Octave2) and the power spectrum of the light curve where the eclipse had been omitted with the automated pipeline developed in Sydney (Huber et al. 2009).

Octave1 computed ν_{max} and $A_{\ell=0}$ (maximum mode amplitude) from a binned power spectrum, and $\Delta\nu$ (large frequency separation) using the power spectrum of the power spectrum. Octave2 computed ν_{max} and $A_{\ell=0}$ from a Gaussian fitting to the oscillation envelope and $\Delta\nu$ from an autocorrelation of the oscillation frequencies. The latter have been determined with a Bayesian method, where oscillation frequencies are those with a posterior probability of less than 0.1% of being noise. The Sydney pipeline produced ν_{max} from a smoothed power spectrum. The current data do not yet allow us to measure the life times of the solar-like oscillations. For more details on the pipelines, we refer to Hekker et al. (2009a) and Huber et al. (2009).

The resulting parameters are listed in Table 2. Note that $A_{\ell=0}$ is computed for a power spectrum with mean squared scaling, which is a factor $\sqrt{2}$ different with respect to the scaling relations of Kjeldsen & Bedding (1995). With the effective temperature and the scaling laws from Kjeldsen & Bedding (1995), we computed the radius, mass, and luminosity of the primary (see Table 2).

We also used the RADIUS pipeline described by Stello et al. (2009) to compute the stellar radius. The input parameters for this pipeline are the large separation, T_{eff} and metallicity, for which we used the spectroscopic values listed in Table 1. The results from this analysis are listed in Table 2 and lead to a value for $\log(g)$ of 2.6 $\pm$ 0.1, which is in agreement with our spectroscopically derived value.

The values computed with different methods and approaches are in good agreement. The weighted mean values of the results from the different methods are used throughout the rest of the paper, i.e., $R_R = 11.8 \pm 0.6 \, R_\odot$, $L_R = 58 \pm 6 \, L_\odot$, $M_R = 1.7 \pm 0.3 \, M_\odot$ (subscript "R" refers to the red giant) together with the

spectroscopically determined effective temperature. We point out that the estimates of these fundamental parameters rely on the input physics of stellar models, through the interpretation of observables (e.g., ν_{max} and $A_{l=0}$) in terms of the properties of the convection and thermodynamics, which we assumed to be known and error-free. This implies that there may be unknown systematic uncertainties. Nevertheless, the radius and mass have values in good agreement with the expected range for red-clump stars. For the radius there is also agreement between the result from scaling relations and from models (RADIUS).

5. BINARY ANALYSIS

The very flat bottom of the eclipse, except for the red giant oscillations, seems to be indicative of a smaller object occulted by a considerably larger object. This is underlined by the fact that for an annular eclipse, i.e., transit, limb darkening effects play a more prominent role and would have caused a more gradually changing shape of the eclipse. Because we have only one eclipse, a full analysis of the binary is not yet possible, but we are able to put several constraints on the nature of the secondary and on the orbit.

From the *Kepler* data, we directly measured the depth of the eclipse to be about 9%. This depth is determined by the luminosity ratio of the two stars, i.e., $l = L_2/L_R = 0.099 \pm 0.005$. The uncertainty is estimated taking the shape of the light curve outside the eclipse into account. In addition to the depth, we measured the time during which the secondary is fully obscured: 1.64 ± 0.01 days. The ingress and egress are symmetric and each lasts for 0.276 ± 0.007 days. The symmetry of the ingress and egress indicates that the relative acceleration of the binary components between ingress and egress is equal to zero, i.e., it is justified to assume the sky-projected relative velocity of the two stars to be constant during the eclipse.

The eclipse time depends on the radii of both stars and the geometry of the system. Knowing that the eclipse lasts only during $\sim$2% or less of the total orbital period, i.e., only a very small segment of the orbit is covered during the eclipse, and that the system is viewed close to the orbital plane, implies that the time of total eclipse (τ_{total}) can be expressed as

$$\tau_{total} = \frac{P(R_R \cos \delta - R_2)}{4a\,E(\epsilon)}, \tag{1}$$

with P being the orbital period, a the semi-major axis, E the complete elliptic integral, ϵ the eccentricity, and δ the latitude of the eclipse on the stellar disk, and R_R and R_2 the radius of the red giant and the secondary, respectively. The total time of ingress, total eclipse and egress ($\tau_{in+total+eg}$) from the same geometric considerations can be expressed as

$$\tau_{in+total+eg} = \frac{P(R_R \cos \delta + R_2)}{4a\,E(\epsilon)}. \tag{2}$$

Dividing Equation (1) by Equation (2) provides an estimate of R_2 as a function of $\cos \delta$:

$$\frac{\tau_{total}}{\tau_{in+total+eg}} \equiv x = \frac{R_R \cos \delta - R_2}{R_R \cos \delta + R_2} = \frac{\cos \delta - r}{\cos \delta + r}, \tag{3}$$

with $r = R_2/R_R$. In this way, we found that

$$\frac{R_2}{R_R} = \cos \delta \frac{1-x}{1+x}, \tag{4}$$

where $x = 0.75 \pm 0.03$. Using $\delta = 0$ (central eclipse) and the value of the radius of the red giant star derived in the previous section, we then find an upper limit of $R_2 \leqslant 1.7 \pm 0.1\,R_\odot$.

To confirm this geometric analysis, we computed a basic model of the eclipse signal. We neglected limb darkening and computed the fractional overlap between the two disks, taking into account the relative luminosity of the star being eclipsed. As explained above, we assumed the sky-projected relative velocity (v) of the two stars to be constant. This model has been fitted to the portion of the light curve near the eclipse using a Markov Chain Monte Carlo approach (see e.g., Torres et al. 2008, and references therein), which yields the joint posterior probability density of all the parameters, given the data.

The physical parameters in our model are r, v, l, and $b = \sin \delta$ (the impact parameter). In order to avoid strong correlations among these parameters (in particular between r, v, and b), when performing the fit we replace v with $v^2/(1-b^2)$ and r with r/v^2. The values of the physical parameters resulting from this fit are $b = 0.0^{+0.15}$, $r = 0.1435^{+0.0008}_{-0.0027}$, $v = 1.0338^{+0.0005}_{-0.011}\,R_R$/day, and $l = 0.10060^{+0.00006}_{-0.00006}$, consistent with the values obtained from the geometric analysis.

To test our assumption that v is constant, we repeated the fit, allowing v to change linearly with time. The result was a deceleration of $0.015^{+0.005}_{-0.004}\,R_R$/day^2 (i.e., $\sim$3% slower at egress than at ingress). This may be a real asymmetry in the eclipse, implying an eccentric orbit. However, it could also be due to the pulsation signal altering the apparent shapes of the ingress and egress.

We converted the fitted value of l into a bolometric luminosity ratio by folding blackbody curves with the *Kepler* spectral response curve. This is a function of the secondary's temperature, as shown in Figure 2 (dot-dashed lines). With the constraint from the radius ratio and

$$\frac{L_2}{L_R} = \frac{R_2^2 T_{eff,2}^4}{R_R^2 T_{eff,R}^4}, \tag{5}$$

we find $L_2 = 5.2 \pm 0.7\,L_\odot$. The secondary is thus probably an F main-sequence star. Using the mass–luminosity relation for stars with masses between 0.5 and 2.0 $M_\odot$, i.e., $(L/L_\odot) = (M/M_\odot)^{4.5}$, we found a mass for the secondary M_2 of $1.44 \pm 0.05\,M_\odot$, where we did not take the uncertainty of the mass–luminosity relation into account. We also computed the surface gravity for the secondary and found $\log(g_2) = 4.2 \pm 0.1$.

The binary also has to obey Kepler's third law:

$$M_R + M_2 = \frac{4\pi^2 a^3}{GP^2}, \tag{6}$$

in which we still have a as unknown, and we take a minimum value of 75 days for P. With this value we computed a minimum semi-major axis for the system of 0.5 AU.

On the other hand, if we assume a circular orbit, we can compute the period. From the eclipse fit, we know the orbital velocity and combining this with Kepler's third law, we get

$$P = \frac{2\pi G(M_R + M_2)}{v^3}. \tag{7}$$

Using the masses of both stars, we obtain $P = 32 \pm 6$ days. This is considerably shorter than the minimum orbital period we inferred from currently available observations, which implies an eccentric orbit.

Table 3
Parameter Overview of Eclipsing Binary KIC8410637

Parameter	Primary	Secondary
R ($R_\odot$)	11.8 ± 0.6	1.7 ± 0.1
L ($L_\odot$)	58 ± 6	5.2 ± 0.7
M ($M_\odot$)	1.7 ± 0.3	1.44 ± 0.05
$T_{\rm eff}$ (K)	4650 ± 80	6700 ± 200
$\log(g)$ (c.g.s.)	2.70 ± 0.15	4.2 ± 0.1
Orbital Parameters		
$P_{\rm orbit}$ (days)	>75	
a (AU)	>0.5	

6. DISCUSSION

From observations obtained with *Kepler*, we found a pulsating red giant in an eclipsing binary. Once a full orbit has been observed, the orbital parameters will provide an independent measure of the stellar parameters, such as mass and radius, with respect to the asteroseismic values. These additional constraints make this a very interesting case, and the star is therefore being followed up by the *Kepler Mission* as well as with ground-based spectroscopy.

Stellar parameters of the primary red giant have been computed from a spectroscopic analysis and from the solar-like oscillations. We did not find evidence of the secondary component in the spectra. The currently available spectra are not yet sufficient to put constraints on the orbit.

From the single eclipse observed by *Kepler* and additional independent observations from TrES, SuperWASP and ASAS, we inferred constraints on the orbit and secondary star. The annular eclipse, i.e., the secondary passing in front of the red giant, would cause an eclipse with a depth of ∼1.7%, assuming a circular orbit and without taking limb-darkening into account. Such a dip would be observable, but has not been detected by *Kepler*, TrES or ASAS. Only the SuperWASP data show a feature that might be due to an annular eclipse. The SuperWASP and ASAS data have gaps due to weather conditions. Although there are also three gaps (4.7, 2.9, and 1.7 days) in the TrES time series data with a duration longer than the duration of the eclipse, we expect the chance that an eclipse falls exactly during one of these gaps to be low. Therefore, we infer that the orbit is longer than the time span of the TrES data, i.e., at least 75 days. Also, an initial inspection of the raw *Kepler* data of Q2 (additional three months of data following the Q1 phase) does not seem to reveal another eclipse. In the case that we missed an eclipse due to a lack of observations, the minimum orbital period would be 135 days.

From the orbital velocity of the secondary, we computed the period for a circular orbit, which would be shorter than half the total time span of the TrES data, and we should have seen an occultation in those data. Therefore, we concluded that the orbit is eccentric. The possible annular eclipse in the SuperWASP data has a length of ∼7 days and depth of ∼0.03 mag. If confirmed this would indeed imply a large orbital eccentricity.

From the eclipse times and depth we were able to compute the luminosity and the radius of the secondary. All values seem to be compatible with an F main-sequence star. The mass–luminosity relation for main-sequence stars then leads to a mass estimate of the secondary as well as its surface gravity. These results are summarized in Table 3, and the positions of both stars are indicated in an H-R diagram in Figure 2.

KIC8410637 is an extremely interesting binary for further follow-up. Longer time series from *Kepler* will improve dramatically the detection threshold for the derivation of the properties of the oscillations of the red giant.

REFERENCES

Baglin, A., et al. 2006, in Proc. *CoRoT* Mission Pre-Launch Status—Stellar Seismology and Planet Finding, ed. M. Fridlund, A. Baglin, J. Lochard, & L. Conroy (ESA SP-1306; Noordwijk: ESA Publications Division), 33
Bedding, T., et al. 2010, ApJ, 713, L176
Blomme, J., et al. 2010, ApJ, 713, L204
Borucki, W., et al. 2009, in IAU Symp. 253, Transiting Planets, ed. F. Pont, D. Sasselov, & M. Holman (Cambridge: Cambridge Univ. Press), 289
Brown, T. M., Everett, M., Latham, D. W., & Monet, D. G. 2005, BAAS, 37, 1340
Debosscher, J., et al. 2009, A&A, 506, 519
De Ridder, J., et al. 2009, Nature, 459, 398
Gilliland, R. L., et al. 2010, PASP, in press (arXiv:1001.0139)
Hekker, S., & Meléndez, J. 2007, A&A, 475, 1003
Hekker, S., et al. 2009a, MNRAS, in press (arXiv:0911.2612)
Hekker, S., et al. 2009b, A&A, 506, 465
Høg, E., et al. 2000, A&A, 355, L27
Huber, D., et al. 2009, CoAst, 160, 74
Kjeldsen, H., & Bedding, T. R. 1995, A&A, 293, 87
Luck, R. E., & Heiter, U. 2007, AJ, 133, 2464
Miglio, A., et al. 2009, A&A, 503, L21
O'Donovan, F. T., et al. 2006, ApJ, 651, L61
Ofek, E. O. 2008, PASP, 120, 1128
Pickles, A. J. 1998, PASP, 110, 863
Pietrinferni, A., Cassisi, S., Salaris, M., & Castelli, F. 2004, ApJ, 612, 168
Pojmański, G. 1997, Acta Astron., 47, 467
Pollacco, D. L., et al. 2006, PASP, 118, 1407
Raskin, G., & Van Winckel, H. 2008, Proc. SPIE, 7014, 70145D
Skrutskie, M. F., et al. 2006, AJ, 131, 1163
Stello, D., et al. 2009, ApJ, 700, 1589
Torres, G., Winn, J. N., & Holman, M. J. 2008, ApJ, 677, 1324